Relativistic nontopological soliton stars in a U(1) gauge Higgs model

Yota Endo,* Hideki Ishihara,† and Tatsuya Ogawa‡

Department of Mathematics and Physics, Graduate School of Science,
Nambu Yoichiro Institute of Theoretical and Experimental Physics (NITEP),
Osaka City University, Osaka 558-8585, Japan

(Received 23 March 2022; accepted 11 April 2022; published 18 May 2022)

We study spherically symmetric nontopological soliton (NTS) stars numerically in the coupled system of a complex scalar field, a U(1) gauge field, a complex Higgs scalar field, and Einstein gravity, where the symmetry is broken spontaneously. The gravitational mass of NTS stars is limited by a maximum mass for a fixed breaking scale, and the maximum mass increases steeply as the breaking scale decreases. In the case of the breaking scale is much less than the Planck scale, the maximum mass of NTS stars becomes the astrophysical scale, and such a star is relativistically compact so that it has the innermost stable circular orbit. The first author contributed with a part of the numerical calculations. The second contributed with planning and conducting the research, and the third contributed with all numerical calculations and finding new properties of the system.

DOI: 10.1103/PhysRevD.105.104041

I. INTRODUCTION

Nontopological solitons (NTSs) are localized solutions carrying a Noether charge in nonlinear field theories that have a continuous global symmetry. Rosen [1], in his pioneering work, showed that a self-interacting complex scalar field theory admits particlelike NTS solutions, and Coleman [2] proved the existence theorem of spherically symmetric NTS solutions with a conserved charge, he called them ‘Q-balls’, in nonlinearly self-coupling complex scalar field theories with some conditions. Friedberg, Lee, and Sirlin [3] studied a coupled system of a complex scalar field and a real scalar field with a double-well potential, and showed the existence of the NTS solutions (see e.g., reviews [4,5] and textbooks [6]). The NTS solutions in extended field theories including a gauge field were also studied in the works [7–9]. The NTSs are interested as a possible candidate of dark matter [10–14], and as sources for baryogenesis [15–17].

Recently, NTS solutions were constructed in the theory that consists of a complex scalar field, a U(1) gauge field, and a complex Higgs scalar field with a Mexican hat potential which causes the spontaneous symmetery breaking [18–20].[1] In this model, there are interesting properties; the charges carried by two scalar fields are screening each other, and NTS solutions with infinitely large mass can exist [20]. These would suggest that NTSs with astrophysical scale in this model can play important roles in cosmology. However, infinite mass should be prohibited if we take gravity produced by the NTS into account, namely, the mass should be limited by a maximum mass for self-gravitating NTSs.

It is also investigated that localized objects are made by self-gravitating complex scalar fields, so-called boson stars. In the model of a free massive complex scalar field with gravity, the gravitational mass of the localized solutions is quite small then the solutions are called miniboson stars [23,24], while if the complex scalar field has nonlinear self-coupling, the mass of the solution can be large [25]. Boson stars in various field models are studied in Refs. [26–28] (see also [29–31] for review). Furthermore, self-gravity of the NTS is also studied in the Coleman’s model [32] and the Friedberg-Lee-Sirlin’s model [33–36].

In this paper we consider the coupled system of two complex scalar fields and a U(1) gauge field, which is studied in Refs. [18–20], with Einstein gravity. The local U(1) symmetry of the system is spontaneously broken in a vacuum state where one of the scalar field has an expectation value. The system has two dimensionful parameters—the symmetry breaking scale, η and the Plank scale, M_{P}—and then the dimensionless parameter η/M_{P} is an important quantity that characterizes the model.

*yota-endo@dt.osaka-cu.ac.jp
†ishihara@osaka-cu.ac.jp
‡taogawa@osaka-cu.ac.jp

[1]NTSs in a generalized model are discussed in Refs. [21,22].

Assuming spherically symmetry, stationary rotation of the phase of complex scalar fields, and static geometry, we derive a set of coupled ordinary differential equations. We obtain numerical solutions that describe self-gravitating objects, we call them 'nontopological soliton stars (NTS stars)' in this paper, and investigate properties of the solutions, especially, mass and radius that depend on η/M_{P}. It is interesting that NTS stars with mass of astrophysical scale are possible, e.g., the solar mass is possible for $\eta \sim 1$ GeV, and the NTS stars can be so compact that they have the innermost stable circular orbits for $\eta/M_{\mathrm{P}} \ll 1$.

The paper is organized as follows. In Sec. II we present the model that has a symmetry breaking scale, and derive basic equations on the assumptions of the geometrical symmetries of the fields. In Sec. III we solve the basic equations numerically, and present NTS star solutions. In Sec. IV we investigate internal structures of the NTS stars; energy density, pressure, and charge density. In Sec. V we study the mass and radius of the NTS stars, and see that the maximum mass appears for each breaking scale. Paying attention to the NTS stars with maximum mass in various breaking scales, we investigate scale dependence of the maximum mass and the compactness in Sec. VI. Section VII is devoted to our conclusions.

II. BASIC MODEL

We consider the action

$$S = \int \sqrt{-g} d^4x \left(\frac{R}{16\pi G} + \mathcal{L}_m \right), \tag{1}$$

where R is the scalar curvature with respect to a metric, $g_{\mu\nu}$, $g \coloneqq \det(g_{\mu\nu})$, and G is the gravitational constant. The matter Lagrangian, $\mathcal{L}_m$, is given by

$$\begin{aligned}\mathcal{L}_m = &-g^{\mu\nu}(D_\mu\psi)^*(D_\nu\psi) - g^{\mu\nu}(D_\mu\phi)^*(D_\nu\phi) - \frac{\lambda}{4}(|\phi|^2 - \eta^2)^2 \\ &-\mu|\phi|^2|\psi|^2 - \frac{1}{4}g^{\mu\alpha}g^{\nu\beta}F_{\mu\nu}F_{\alpha\beta},\end{aligned} \tag{2}$$

where it consists of a complex matter scalar field ψ, the field strength $F_{\mu\nu} \coloneqq \partial_\mu A_\nu - \partial_\nu A_\mu$ of a U(1) gauge field A_μ, and a complex Higgs scalar field ϕ. The gauge field couples to the scalar fields through the gauge covariant derivative, $D_\mu \coloneqq \partial_\mu - ieA_\mu$. The parameter e is the charge of the fields ψ and ϕ, λ the Higgs self-coupling, μ the Higgs-scalar coupling, and η the Higgs vacuum expectation value determining the scale of the symmetry breaking.

The Lagrangian (2) has local $\mathrm{U}(1) \times$ global $\mathrm{U}(1)$ symmetry under the gauge transformation given by

$$\psi(x) \to \tilde{\psi}(x) = e^{i(\chi(x)-\gamma)}\psi(x), \tag{3}$$

$$\phi(x) \to \tilde{\phi}(x) = e^{i(\chi(x)+\gamma)}\phi(x), \tag{4}$$

$$A_\mu(x) \to \tilde{A}_\mu(x) = A_\mu(x) + e^{-1}\partial_\mu\chi(x), \tag{5}$$

where $\chi(x)$ is an arbitrary function that depends on spacetime coordinate, and γ is an arbitrary constant. Concerning this invariance, conserved currents,

$$\begin{aligned} j^\mu_\psi &\coloneqq ie(\psi^*(D^\mu\psi) - (D^\mu\psi)^*\psi), \\ j^\mu_\phi &\coloneqq ie(\phi^*(D^\mu\phi) - (D^\mu\phi)^*\phi), \end{aligned} \tag{6}$$

and conserved charges

$$Q_\psi \coloneqq \int d^3x\sqrt{-g}\rho_\psi, \qquad Q_\phi \coloneqq \int d^3x\sqrt{-g}\rho_\phi, \tag{7}$$

are defined, where $\rho_\psi \coloneqq j^t_\psi$ and $\rho_\phi \coloneqq j^t_\phi$ are charge densities induced by the complex scalar field ψ and ϕ, respectively. The integrations in (7) are performed on a time slice, $t = \mathrm{const}$.

Owing to the potential term of the complex Higgs scalar field ϕ in (2), ϕ takes a nonzero vacuum expectation value η in a vacuum state. As a result, the symmetry is spontaneously broken. Then, the scalar field ψ and the U(1) gauge field A_μ acquire masses, $m_\psi \coloneqq \sqrt{\mu}\eta$ and $m_A \coloneqq \sqrt{2}e\eta$, respectively, through interactions with the complex Higgs field. Simultaneously, a real scalar field as a fluctuation of the amplitude of ϕ around η also acquires the mass $m_\phi \coloneqq \sqrt{\lambda}\eta$.

From the action (1), we can derive field equations

$$\frac{1}{\sqrt{-g}}D_\mu(\sqrt{-g}g^{\mu\nu}D_\nu\psi) - \mu\psi|\phi|^2 = 0, \tag{8}$$

$$\frac{1}{\sqrt{-g}}D_\mu(\sqrt{-g}g^{\mu\nu}D_\nu\phi) - \frac{\lambda}{2}\phi(|\phi|^2 - \eta^2) - \mu|\psi|^2\phi = 0, \tag{9}$$

$$\frac{1}{\sqrt{-g}}\partial_\mu(\sqrt{-g}F^{\mu\nu}) = j^\nu_\psi + j^\nu_\phi, \tag{10}$$

$$G_{\mu\nu} = 8\pi G T_{\mu\nu}, \tag{11}$$

where $G_{\mu\nu} \coloneqq R_{\mu\nu} - \frac{1}{2}g_{\mu\nu}R$ is the Einstein tensor and $T_{\mu\nu}$ is the energy-momentum tensor given by

$$\begin{aligned} T_{\mu\nu} &\coloneqq -\frac{2}{\sqrt{-g}}\frac{\delta(\sqrt{-g}\mathcal{L}_m)}{\delta g^{\mu\nu}} \\ &= 2(D_\mu\psi)^*(D_\nu\psi) - g_{\mu\nu}(D_\alpha\psi)^*(D^\alpha\psi) \\ &\quad + 2(D_\mu\phi)^*(D_\nu\phi) - g_{\mu\nu}(D_\alpha\phi)^*(D^\alpha\phi) \\ &\quad - g_{\mu\nu}\left(\frac{\lambda}{4}(|\phi|^2 - \eta^2)^2 + \mu|\psi|^2|\psi|^2\right) \\ &\quad + \left(F_{\mu\alpha}F^\alpha_\nu - \frac{1}{4}g_{\mu\nu}F_{\alpha\beta}F^{\alpha\beta}\right). \end{aligned} \tag{12}$$

Here, we assume stationary and spherically-symmetric fields in the form,

$$\psi = e^{-i\omega t}u(r), \quad \phi = e^{-i\omega' t}f(r), \quad A = A_t(r)dt, \tag{13}$$

where we use a spherical coordinate (t, r, θ, φ). The parameters ω and ω' are constant angular frequencies of the complex scalar fields. Owing to the gauge transformation (3)–(5), we can fix the variables as

$$\begin{aligned}
&\phi(r) \to f(r), \qquad \psi(t,r) \to e^{i\Omega t}u(r),\\
&A_t(r) \to \alpha(r) \coloneqq A_t(r) + e^{-1}\omega',
\end{aligned} \tag{14}$$

where $\Omega \coloneqq \omega' - \omega$ is the parameter which characterizes the solution, and takes a positive value without loss of generality.

We also take static and spherically symmetric spacetime assumptions in the form

$$\begin{aligned}
ds^2 &= g_{\mu\nu}dx^\mu dx^\nu\\
&= -\sigma(r)^2\left(1 - \frac{2m(r)}{r}\right)dt^2 + \left(1 - \frac{2m(r)}{r}\right)^{-1}dr^2\\
&\quad + r^2 d\theta^2 + r^2\sin^2\theta d\varphi^2,
\end{aligned} \tag{15}$$

where $\sigma(r)$ and $m(r)$ are functions of r. Note that $\sigma(r)$ is dimensionless, and $m(r)$ has dimension of length. The Einstein equations reduce to

$$\begin{aligned}
&G^t_t = 8\pi G T^t_t, \qquad G^r_r = 8\pi G T^r_r,\\
&G^\theta_\theta = G^\varphi_\varphi = 8\pi G T^\theta_\theta = 8\pi G T^\varphi_\varphi.
\end{aligned} \tag{16}$$

Substituting assumptions (14) and (15) into (8)–(10), we obtain equations for the fields ψ, ϕ, and A to be solved in the form,

$$\begin{aligned}
&u'' + \left(\frac{2}{r}\left(1 + \frac{m - rm'}{r - 2m}\right) + \frac{\sigma'}{\sigma}\right)u'\\
&\quad + \left(1 - \frac{2m}{r}\right)^{-1}\left(\frac{(e\alpha - \Omega)^2 u}{\sigma^2(1 - 2m/r)} - \mu f^2 u\right) = 0,
\end{aligned} \tag{17}$$

$$\begin{aligned}
&f'' + \left(\frac{2}{r}\left(1 + \frac{m - rm'}{r - 2m}\right) + \frac{\sigma'}{\sigma}\right)f'\\
&\quad + \left(1 - \frac{2m}{r}\right)^{-1}\left(\frac{e^2 f\alpha^2}{\sigma^2(1 - 2m/r)} - \frac{\lambda}{2}f(f^2 - 1) - \mu f u^2\right) = 0,
\end{aligned} \tag{18}$$

$$\begin{aligned}
&\alpha'' + \left(\frac{2}{r} - \frac{\sigma'}{\sigma}\right)\alpha'\\
&\quad + \left(1 - \frac{2m}{r}\right)^{-1}(-2e^2 f^2\alpha - 2e(e\alpha - \Omega)u^2) = 0,
\end{aligned} \tag{19}$$

where the prime denotes the derivative with respect to r. Here and hereafter, r, $u(r)$, $f(r)$, $\alpha(r)$, $m(r)$, and Ω are normalized by η.

As for the Einstein equations, we solve the time-time component of (16) and the combination

$$G^r_r - G^t_t = 8\pi G(T^r_r - T^t_t). \tag{20}$$

The rest is guaranteed by the Bianchi identity. Explicit forms of the energy-momentum tensor and the charge densities are given in the Appendix. Then, we have

$$\begin{aligned}
&\frac{2m'}{r^2} - 8\pi G\eta^2\left(\frac{e^2 f^2\alpha^2}{\sigma^2(1 - 2m/r)} + \frac{(e\alpha - \Omega)^2 u^2}{\sigma^2(1 - 2m/r)}\right.\\
&\quad + \left(1 - \frac{2m}{r}\right)(f'^2 + u'^2)\\
&\quad \left. + \frac{\lambda}{4}(f^2 - 1)^2 + \mu f^2 u^2 + \frac{1}{2\sigma^2}\alpha'^2\right) = 0,
\end{aligned} \tag{21}$$

and

$$\begin{aligned}
&\frac{(1 - 2m/r)\sigma'}{r\sigma} - 8\pi G\eta^2\left(\frac{e^2 f^2\alpha^2}{\sigma^2(1 - 2m/r)} + \frac{(e\alpha - \Omega)^2 u^2}{\sigma^2(1 - 2m/r)}\right.\\
&\quad \left. + \left(1 - \frac{2m}{r}\right)(f'^2 + u'^2)\right) = 0.
\end{aligned} \tag{22}$$

The dimensionless parameter $G\eta^2 = (\eta/M_{\mathrm{P}})^2$ represents the symmetry-breaking scale with respect to the Planck mass, M_{P}. In the limiting case of $G\eta^2 \to 0$, the gravitational field decouples with the matter fields, where the matter system (17)–(19) with $\sigma(r) = 1$ and $m(r) = 0$ are studied in Refs. [18–20].

We require regularity of the spherically-symmetric fields at the origin described by

$$\sigma' = 0, \quad m = 0, \quad u' = 0, \quad f' = 0, \quad \alpha' = 0. \tag{23}$$

In addition, we assume that the solutions are localized in finite regions. Therefore, for the matter fields, we assume

$$u = 0, \qquad f = 1, \quad \alpha = 0, \tag{24}$$

at spatial infinity. The energy-momentum tensor $T_{\mu\nu}$ of the matter fields satisfying (23) and (24) is localized in a neighborhood of the origin with a quick radial decay, then we require that the gravitational fields satisfy

$$\sigma = 1, \qquad m = m_\infty = \text{const.} \tag{25}$$

at spatial infinity.

III. NUMERICAL CALCULATIONS

In this section, we obtain solutions by solving the set of equations (17), (18), (19), (21), and (22), numerically, and study properties of the numerical solutions. In this article we fix the coupling constants as $e = 1.0$, $\mu = 1.4$, and

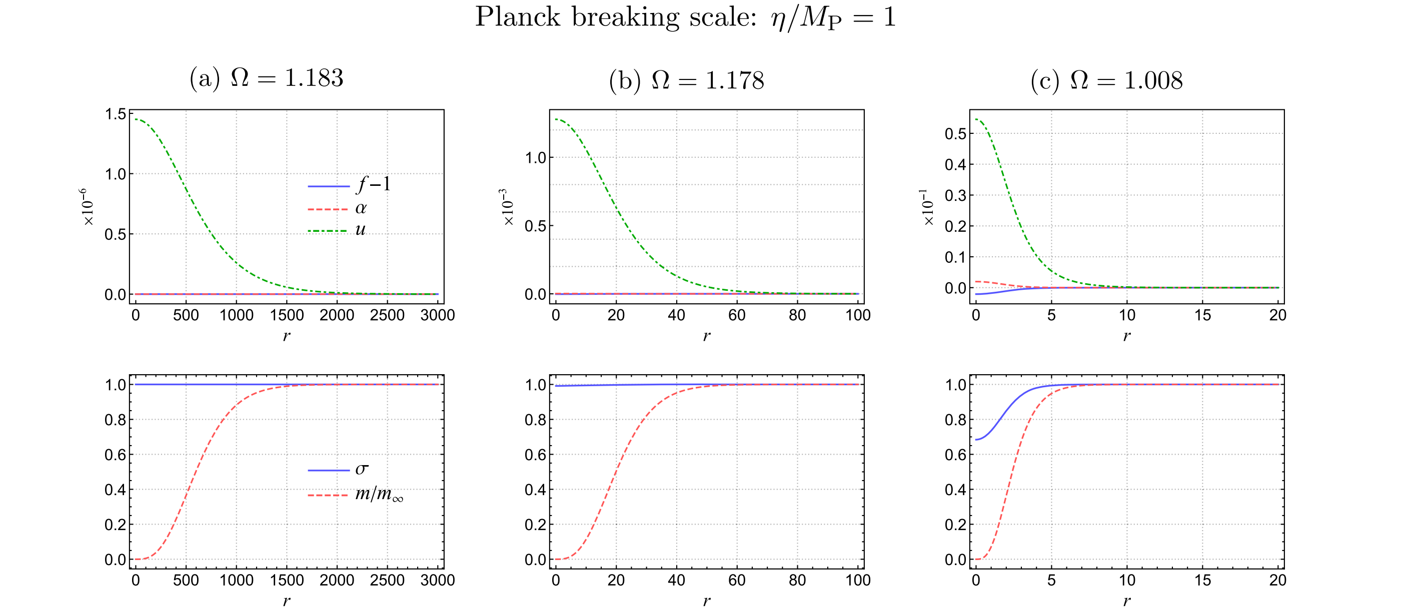

FIG. 1. Field configurations of numerical solutions in the Planck breaking scale case $\eta/M_P = 1$. We show three subcases of the parameter: (a) $\Omega = 1.183$ (left column), (b) $\Omega = 1.178$ (middle column), and (c) $\Omega = 1.008$ (right column). The scalar fields u, f, and the gauge field α are plotted in the upper panels, and the metric components σ and m are plotted in the lower panels.

$\lambda = 1.0$, for an example. On the other hand, we consider various symmetry breaking scales. For the Planck breaking scale, $\eta/M_P = 1$, we have $m_\psi \sim m_\phi \sim m_A \sim 10^{19}$ GeV, and for the lower breaking scale, $\eta/M_P = 10^{-3}$, $m_\psi \sim m_\phi \sim m_A \sim 10^{16}$ GeV, respectively.

At a large distance, $u(r)$ should decrease quickly so that the energy is localized in a compact region. The boundary conditions at the spatial infinity, (24) and (25), require $f = 1$, $\alpha = 0$, and $\sigma = 1$, $m =$ const, then Eq. (17) for $u(r)$ reduces to

$$u'' - (\mu - \Omega^2)u = 0. \tag{26}$$

Then, Ω is bounded above by $\Omega_{\max} \coloneqq \sqrt{\mu}$. For the existence of a solution, there is also the lower bound $\Omega_{\min}$ that depends on η/M_P. As is seen later, the solution has the maximum mass for Ω near $\Omega_{\min}$. We can find numerical solutions for the parameter Ω in the range

$$\Omega_{\min} \le \Omega < \Omega_{\max}. \tag{27}$$

Typical behaviors of the fields obtained by numerical calculations are shown as functions of r in Fig. 1 for the Planck breaking-scale case, and in Fig. 2 for the lower breaking-scale case. They show that the matter fields and the gravitational field are localized in a finite region in each case. Thus, they represent nontopological solitons with self-gravity, we call them nontopological soliton star (NTS star) solutions.

In the cases (a) and (b) in the Planck breaking scale, and (d) in the lower breaking scale, the function u has a Gaussian form in each case, while $f \sim 1$ and $\alpha \sim 0$ almost everywhere. In these cases, the scalar field ϕ and the gauge field A are not excited anywhere, and only the scalar field ψ, which has the mass $m = m_\psi$ by the Higgs mechanism, becomes a source of gravity. The behavior that the massive scalar field with gravity yields compact objects is just the same as 'miniboson star' solutions [23,24]. On the other hand, in the cases (e) and (f) in the lower breaking scale, ψ, ϕ, and A are exited inside the stars. In these cases, interaction between the scalar fields and the gauge field plays an important role for the appearance of solutions [18–20].

As for the gravity, in the cases (a), (b), (d), and (e), the lapse function, σ, is almost constant. It means that the gravity is weak so that the Newtonian description is possible. In contrast, in the cases (c) and (f), σ varies significantly from $r = 0$ to infinity, i.e., it means the gravity requires a relativistic description. Paying attention to the scale of the horizontal axis, we see the size of the NTS stars depend on Ω. This dependence is discussed later in detail.

IV. ENERGY DENSITY, PRESSURE, AND CHARGE DENSITIES

A. Energy density and pressure

The energy density and the pressure, defined by (A1)–(A3) in Appendix, are plotted in Fig. 3 for numerical solutions. We see that the pressures can be ignored compared to the energy density in the cases (a), (b) in the Planck breaking-scale case, and in the cases (d) and (e) in the lower breaking-scale case. Then, NTS stars in these cases behave as 'gravitating dust balls'. On the other

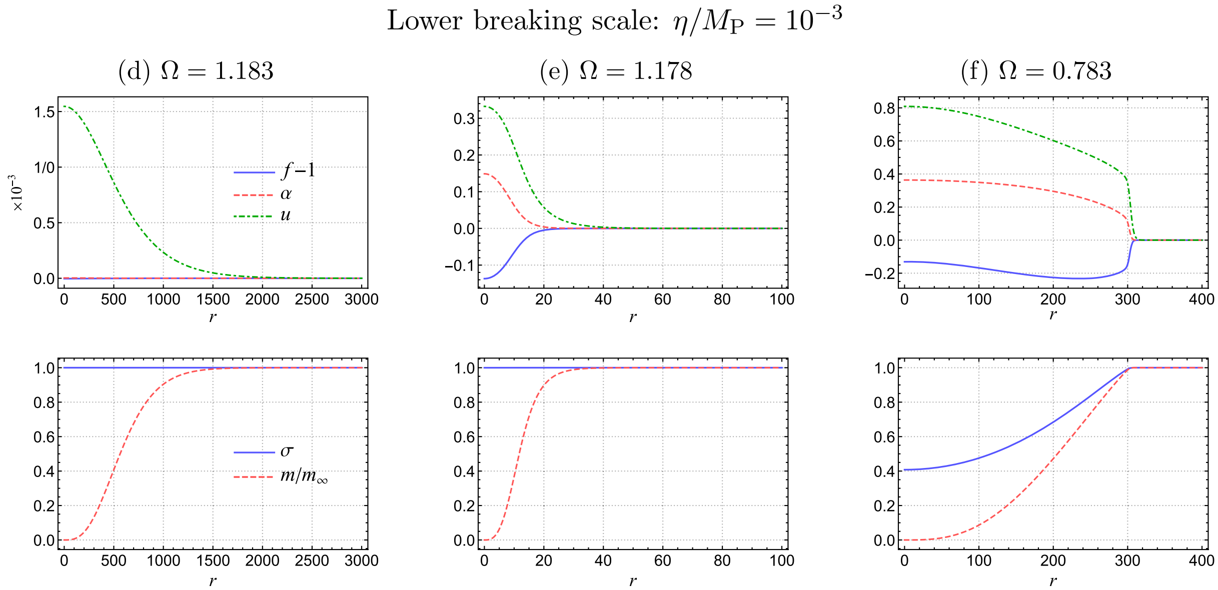

FIG. 2. The same ones as Fig. 1 in the lower breaking scale, $\eta/M_{\mathrm{P}} = 10^{-3}$. We show for (d) $\Omega = 1.183$ (left column), (e) $\Omega = 1.178$ (middle column), and (f) $\Omega = 0.783$ (right column).

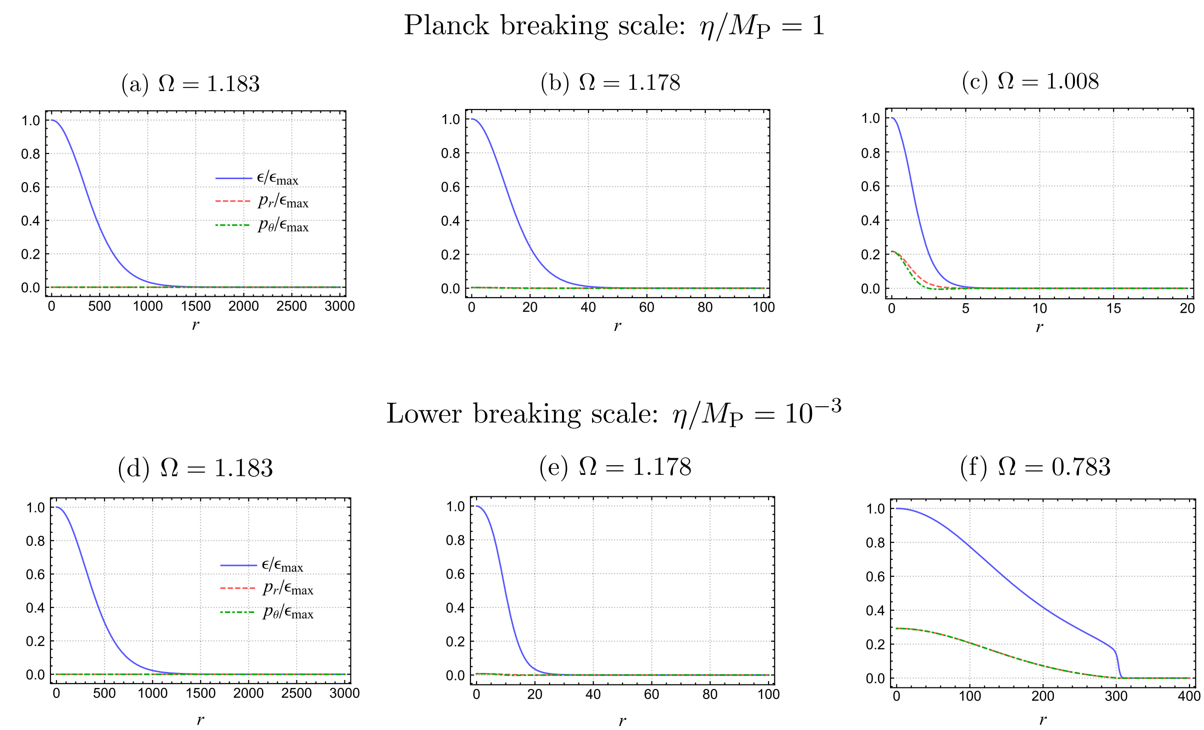

FIG. 3. The energy density ϵ, the radial pressure p_r, and the tangential pressure p_θ, where ϵ_{max} is the maximum value of ϵ. The upper panels correspond to the Planck breaking-scale case, $\eta/M_{\mathrm{P}} = 1$, and the lower does the lower breaking-scale case, $\eta/M_{\mathrm{P}} = 10^{-3}$.

hand, in the cases (c) and (f), the radial and tangential pressures become large in the central regions.

B. Charge distribution

We plot the charge density of ψ, ρ_ψ, and charge density of ϕ, ρ_ϕ, and total one $\rho_{\mathrm{total}} = \rho_\psi + \rho_\phi$ of the NTS stars in Fig. 4. In all cases except (c), ρ_ψ is compensated by ρ_ϕ then charge screening occurs everywhere [18]. In case (c), ρ_{total} is positive in the central region, and negative surrounding the region. Total charge, integration of ρ_{total} from $r = 0$ to the large r, vanishes. Namely, the charge is totally screened. This fact is consistent with the gauge field, A, becoming massive, and α decays quickly as $r \to \infty$.

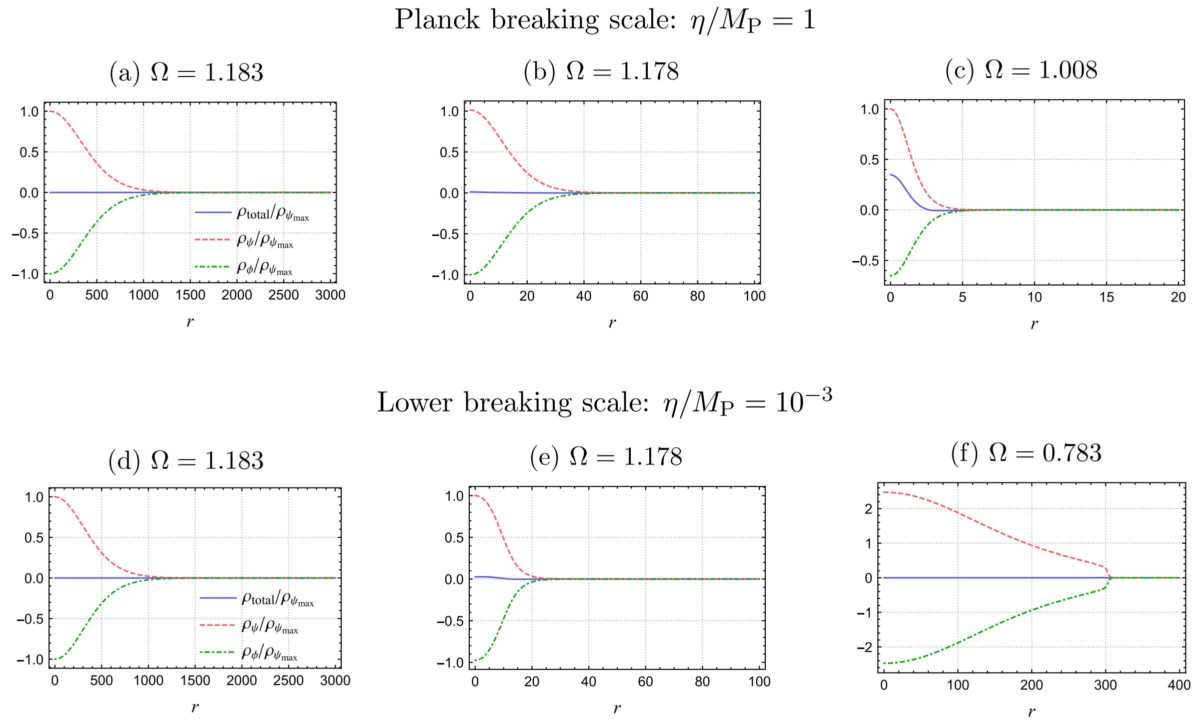

FIG. 4. The charge densities ρ_ψ, ρ_ϕ, and the total charge density $\rho_{\rm total} = \rho_\psi + \rho_\phi$ are plotted, where these charge densities are normalized by the maximum value of ρ_ψ. The upper panels correspond to the Planck breaking-scale case, $\eta/M_{\rm P} = 1$, and the lower does the lower breaking-scale case, $\eta/M_{\rm P} = 10^{-3}$.

V. MASS AND RADIUS

We see in Figs. 1–3, that the size of NTS solutions depend on the parameter Ω. We study the total mass and radius of the solutions in this section.

A. Gravitational mass

The gravitational mass of the NTS star, M_G, is given by

$$M_G = \frac{m_\infty}{G\eta}. \tag{28}$$

For a fixed $\eta/M_{\rm P}$ we have a NTS star solution for each Ω, then M_G is a function of Ω. In Fig. 5, the curves represent M_G as functions of Ω for various breaking scales $\eta/M_{\rm P}$. We find each curve has a spiral shape at the left end. Then there appears lower limit of Ω, $\Omega_{\rm min}$, for the existence of NTS star solutions. Numerically, we have $\Omega_{\rm min} \sim 0.91$ for $\eta/M_{\rm P} \gtrsim 10^{-1}$, while $\Omega_{\rm min} \sim 0.765$ for $\eta/M_{\rm P} \lesssim 10^{-2}$. The gravitational mass M_G is multivalued in Ω near a region $\Omega \sim \Omega_{\rm min}$. For a fixed $\eta/M_{\rm P}$, there exists maximum of M_G near $\Omega \sim \Omega_{\rm min}$. We call the NTS star with the maximum mass 'the maximum NTS star'. The maximum NTS stars for $\eta/M_{\rm P} = 10^{-3}$ and $\eta/M_{\rm P} = 1$ are marked by asterisks in Fig. 5. In Fig. 3 the central pressure in the maximum NTS star cases, (c) and (f), become large in the order of $1/4 \sim 1/3$ times the central energy density. The pressure gradient balances to the gravitational force by the large mass.

For $\eta/M_{\rm P} \gtrsim 10^{-1}$, the curves are shifted upward, as a whole, as $\eta/M_{\rm P}$ decreases, while for $\eta/M_{\rm P} \lesssim 10^{-2}$, the curves are modified, and middle part of the curves converge to the limiting curve of $\eta/M_{\rm P} = 0$. Let us pay attention to the curve of $\eta/M_{\rm P} = 10^{-3}$, for example see Fig. 6. The curve is divided into three parts: the middle segment that lies on the limiting curve $\eta/M_{\rm P} = 0$, the right segment downward from the limiting curve, the left segment leftward from the limiting curve. Firstly, solutions on the right segment are 'miniboson stars' as mentioned before. Secondly, solutions on the middle are NTS stars whose gravity can be neglected, while the interaction of the scalar fields and the gauge field is important, then we call them 'matter-interacting NTS stars'. Thirdly, solutions on the left segment are NTS stars whose gravity is important; we call them 'gravitating NTS stars'. In the family of the gravitating NTS stars, the mass quickly increases as Ω approaches $\Omega_{\rm min}$. The points (a)–(f) on the curves in Fig. 5 correspond to the solutions shown in Figs. 1 and 2, respectively.

B. Surface radius

We define the surface radius of the numerical solutions, r_s, by

$$m(r_s) \coloneqq 0.99 m_\infty. \tag{29}$$

Namely, 99% of total mass of the NTS stars includes within the surface radius r_s. We plot gravitational mass M_G of the

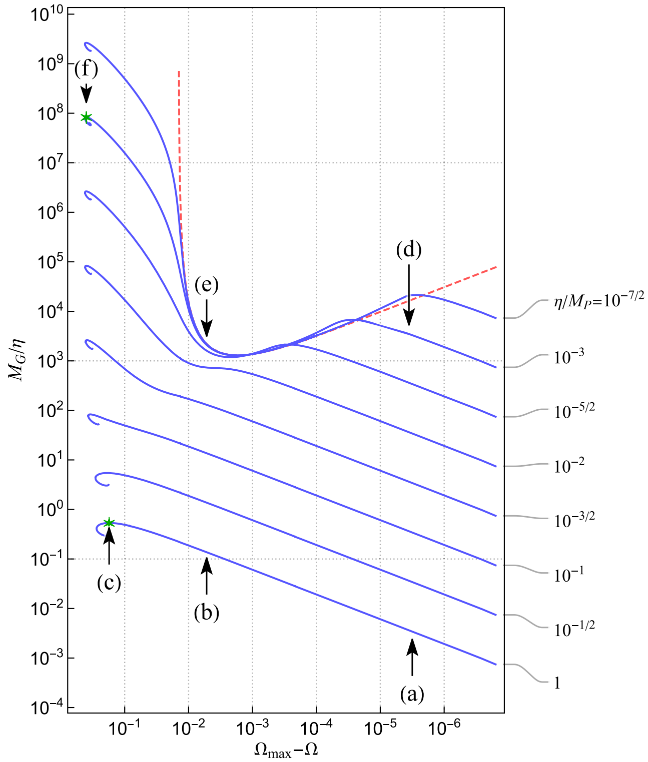

FIG. 5. The gravitational mass of NTS stars as a function of Ω for various breaking scales η/M_P. The vertical axis is taken for M_G/η and the horizontal axis for $\log(\Omega_{max} - \Omega)$. The (red) broken curve denotes the mass of NTS solutions, dust balls [19,20], decouple to gravity, i.e., $\eta/M_P \to 0$. The points (a)–(f) correspond to the solutions shown in Figs. 1–4.

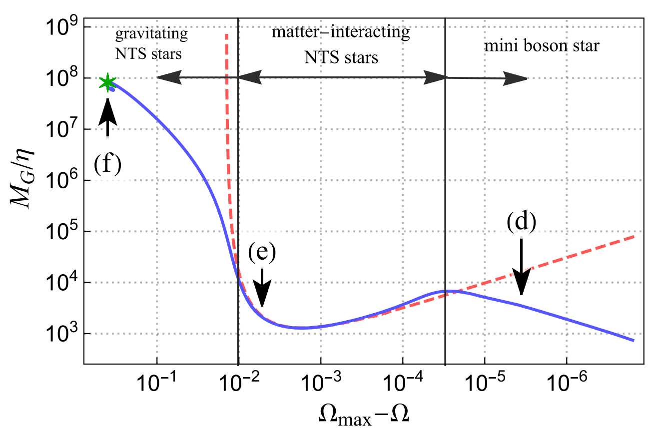

FIG. 6. The gravitational mass of NTS stars for the lower breaking scales $\eta/M_P = 10^{-3}$. In this case the NTS star solutions are classified into three types: miniboson stars, matter-interacting NTS stars, and gravitating NTS stars.

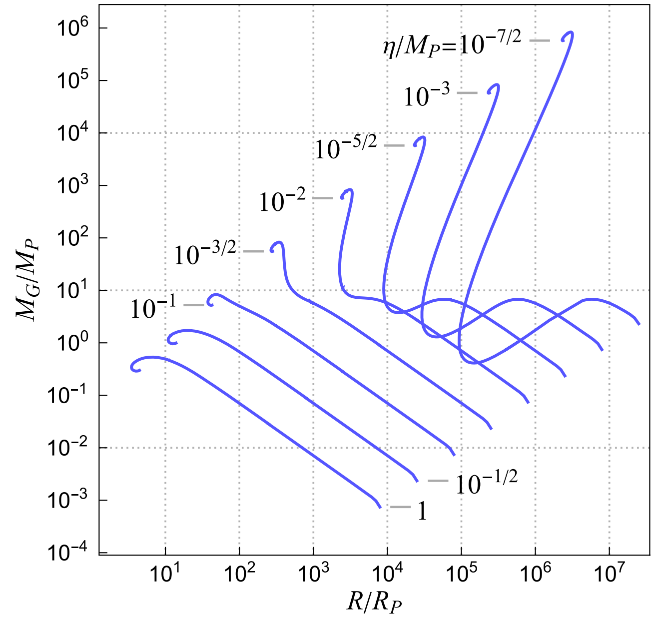

FIG. 7. The gravitational mass M_G of the NTS stars as a function of surface radius R for various breaking scales. On the vertical axis M_G is normalized by the Planck mass M_P, and in the horizontal axis R is normalized by the Planck length $R_P \coloneqq \sqrt{G}$.

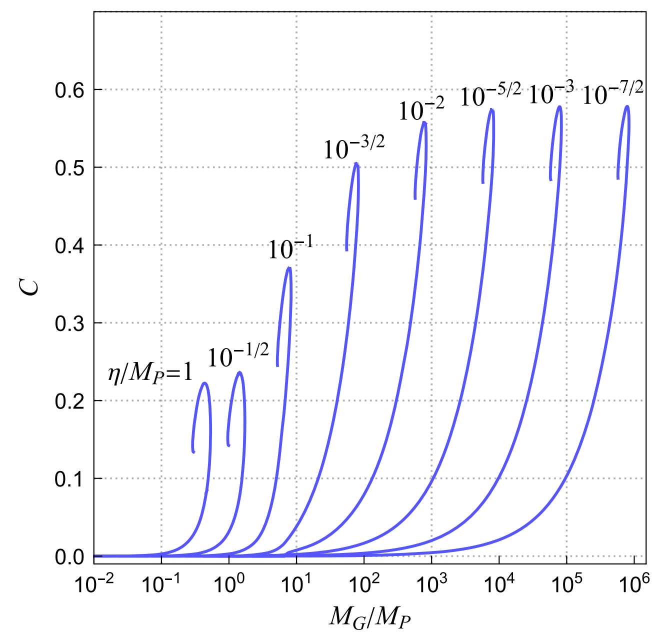

FIG. 8. The compactness of NTS stars as a function of the gravitational mass M_G for various breaking scales.

NTS stars normalized by M_P as a function of dimensionful radius $R \coloneqq r_s/\eta$ for various breaking scales in Fig. 7. For a fixed breaking scale in the range $\eta/M_P \gtrsim 10^{-1}$, M_G increases toward the maximum mass as R decreases, while in the range $\eta/M_P \lesssim 10^{-5/2}$, M_G depends on R in a complicated way; in the region $M_G/M_P \lesssim 10$, a local maximum and a local minimum appear and in the region $M_G/M_P \gtrsim 10$, M_G increases toward the maximum mass as R increases.

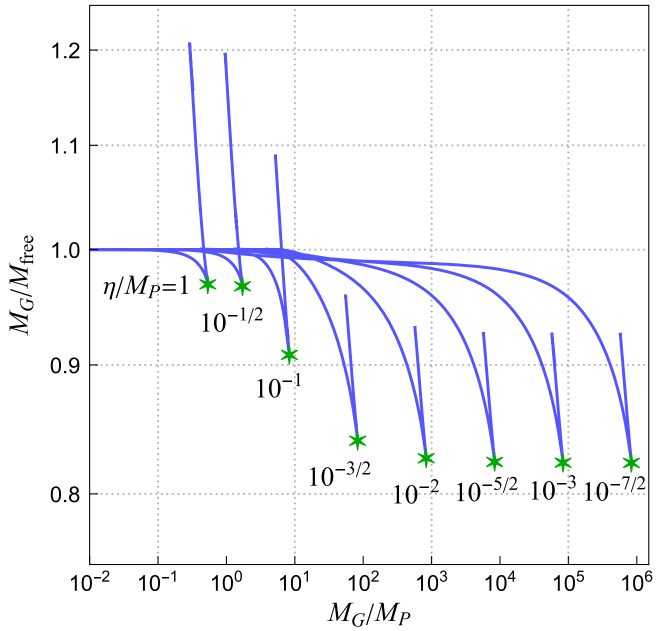

FIG. 9. The mass ratio $M_G/M_{\rm free}$ as a function of M_G for various breaking scales. The asterisk mark represents the maximum NTS solution for each breaking scale.

C. Compactness

Next, we investigate the compactness, C, defined by

$$C \coloneqq \frac{2GM_G}{R} = \frac{2m_\infty}{r_s}. \tag{30}$$

In Schwarzschild geometries, which are the exterior of NTS stars, if $C \geq 2/3$ there exists the photon sphere and if $C \geq 1/3$ the innermost stable circular orbit (ISCO) appears.

In Fig. 8 we show the compactness C of the NTS stars as a function of the gravitational mass M_G for various breaking scales. For a fixed breaking scale, C increases monotonically towards the maximum value as M_G increases. The maximum value of C depends on the breaking scale; $C < 1/3$ for $\eta/M_{\rm P} \gtrsim 10^{-1/2}$ and $C > 1/3$ for $\eta/M_{\rm P} \lesssim 10^{-1}$. In the latter case a NTS star can be so compact that the star has ISCO around it.

D. Binding Energy

Here, we consider stability of the NTS stars in terms of the binding energy defined by $B_G \coloneqq M_G - M_{\rm free}$, where $M_{\rm free}$ is sum of mass of free ψ particles that carry totally the same charge Q_ψ of the NTS stars. A NTS star with $B_G > 0$, ($M_G/M_{\rm free} > 1$), would disperse into free particles, i.e., the NTS star is energetically unstable, while a NTS star with $B_G < 0$, ($M_G/M_{\rm free} < 1$), is stable against dispersion.

In Fig. 9 we plot the mass ratio, $M_G/M_{\rm free}$, as a function of M_G for various breaking scales. The asterisk marks represent the maximum NTS solutions. It shows that the maximum NTS stars in all breaking scales have maximum negative binding energies where $M_G/M_{\rm free} < 1$, then solutions near the maximum NTS stars are stable in all breaking scales.

VI. BREAKING SCALE DEPENDENCE

As shown in the previous section, in each breaking scale there exists a maximum NTS star that has maximum gravitational mass. The mass, the surface radius, and the compactness of the maximum NTS star much depend on the breaking scale. Here, we show how these properties of the maximum NTS star depend on the breaking scale.

In Fig. 10 we plot the mass, M_*, and the surface radius, R_*, of the maximum NTS stars for the various values of the breaking scale $\eta/M_{\rm P}$. We observe that the both M_* and R_* obey power laws of $\eta/M_{\rm P}$ with two different power indices as

$$\frac{M_*}{M_{\rm P}} \propto \begin{cases} \left(\frac{\eta}{M_{\rm P}}\right)^{-2} & \text{for } \eta < \eta^M_{\rm cr}, \\ \left(\frac{\eta}{M_{\rm P}}\right)^{-1} & \text{for } \eta > \eta^M_{\rm cr}, \end{cases} \tag{31}$$

and

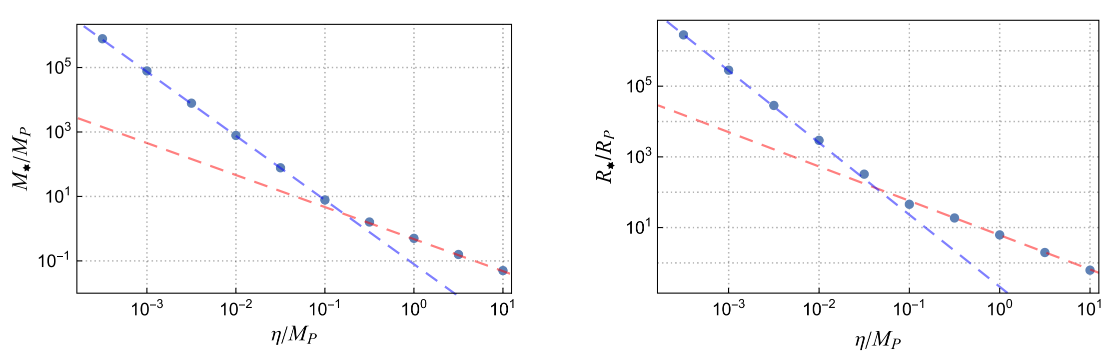

FIG. 10. The mass of the maximum NTS stars (left panel), and the surface radius (right panel) for each breaking scale $\eta/M_{\rm P}$ are plotted as dots. The plots are fitted by double power laws, respectively.

TABLE I. The mass, M_*, and the radius, R_*, of the maximum NTS star for various breaking scales. The symbol $M_\odot$ denotes the solar mass.

Symmetry breaking scale	M_* [kg]	R_*[m]
$\eta \sim 10^{19}$ GeV	$\mathcal{O}(10^{-8})$	$\mathcal{O}(10^{-35})$
$\eta \sim 10^{16}$ GeV	$\mathcal{O}(10^{-2})$	$\mathcal{O}(10^{-29})$
$\eta \sim 10^{2}$ GeV	$\mathcal{O}(10^{26})$	$\mathcal{O}(10^{-1})$
$\eta \sim 1.0$ GeV	$\mathcal{O}(10^{30}) \sim M_\odot$	$\mathcal{O}(10^{3})$
$\eta \sim 1.0$ MeV	$\mathcal{O}(10^{6}\ M_\odot)$	$\mathcal{O}(10^{9})$
$\eta \sim 1.0$ keV	$\mathcal{O}(10^{12}\ M_\odot)$	$\mathcal{O}(10^{15})$
$\eta \sim 1.0$ eV	$\mathcal{O}(10^{18}\ M_\odot)$	$\mathcal{O}(10^{21})$

$$\frac{R_*}{R_\mathrm{P}} \propto \begin{cases} (\frac{\eta}{M_\mathrm{P}})^{-2} & \text{for } \eta < \eta_\mathrm{cr}^R, \\ (\frac{\eta}{M_\mathrm{P}})^{-1} & \text{for } \eta > \eta_\mathrm{cr}^R, \end{cases} \tag{32}$$

where the critical values η_cr^M and η_cr^R are order of $0.1 M_\mathrm{P}$, and the ratio is $\eta_\mathrm{cr}^M/\eta_\mathrm{cr}^R \sim 3.3$. The power index in $\eta \gg \eta_\mathrm{cr}$ is the same as miniboson stars studied in [23,24], and the one in $\eta \ll \eta_\mathrm{cr}$ is the same as soliton stars studied in [34,35].

We consider simple model formulas for M_* and R_* shown in Fig. 10 as

$$M_* = \frac{M_\mathrm{cr}}{2}((\eta/\eta_\mathrm{cr}^M)^{-2} + (\eta/\eta_\mathrm{cr}^M)^{-1}), \tag{33}$$

$$R_* = \frac{R_\mathrm{cr}}{2}((\eta/\eta_\mathrm{cr}^R)^{-2} + (\eta/\eta_\mathrm{cr}^R)^{-1}), \tag{34}$$

where M_cr and R_cr are constants. If we can extrapolate (33) and (34) for much lower breaking scales than the cases calculated in the present paper, typical scales of M_* and R_* for the maximum NTS stars are listed in Table I. We see that the maximum NTS star would be an astrophysical scale for $\eta \lesssim 100$ GeV.

According to the model functions (33) and (34), we have

$$C_* = \frac{2GM_*}{R_*} = \frac{2GM_\mathrm{cr}}{R_\mathrm{cr}} \frac{\eta_\mathrm{cr}^M}{\eta_\mathrm{cr}^R} \frac{(\eta_\mathrm{cr}^M + \eta)}{(\eta_\mathrm{cr}^R + \eta)}, \tag{35}$$

then C_* takes the different constant values for $\eta \ll \eta_\mathrm{cr}$ and $\eta \gg \eta_\mathrm{cr}$, respectively, and the ratio of them becomes

$$\frac{C_*(\eta \ll \eta_\mathrm{cr})}{C_*(\eta \gg \eta_\mathrm{cr})} = \frac{\eta_\mathrm{cr}^M}{\eta_\mathrm{cr}^R} \sim 3.3. \tag{36}$$

In Fig. 11, we depict the compactness of the maximum NTS stars, C_*, by the use of the numerical values of M_* and R_* as a function of the breaking scale. From numerical results we see $C_* \sim 0.553$ for $\eta/M_\mathrm{P} \lesssim 10^{-2}$ and $C_* \sim 0.167$ for $\eta/M_\mathrm{P} \gtrsim \eta_\mathrm{cr}$. Therefore, the maximum NTS stars in $\eta \ll \eta_\mathrm{cr}$ are relativistic self-gravitating objects that have innermost stable circular orbits but no photon sphere.

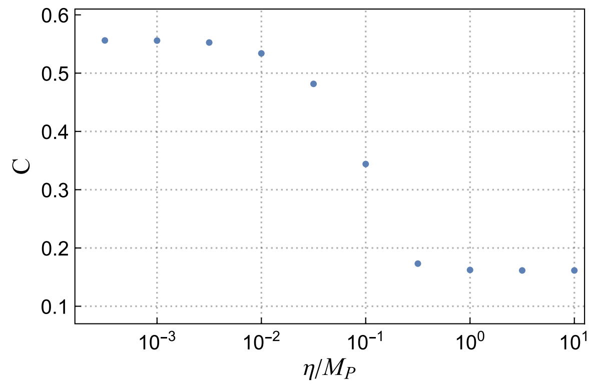

FIG. 11. The compactness of the maximum NTS stars for various breaking scales.

VII. CONCLUSIONS

We studied the coupled system of field theory that consists of a complex scalar field, a U(1) gauge field, a complex Higgs scalar field that causes a spontaneous symmetry breaking, and Einstein gravity. The system has a dimensionless parameter, η/M_P, which represents the ratio of the symmetry breaking scale to the Plank scale. We obtained numerical solutions that describe nontopological soliton stars, parametrized by the angular phase velocity of the complex scalar field, Ω. The solutions have a variety of properties depending on the parameters η/M_P and Ω.

In the case of the large breaking scale, $\eta/M_\mathrm{P} \gtrsim 0.1$, the solutions are almost determined by the gravitational field and a scalar field that acquires its mass by the Higgs mechanism. Then, the solutions are almost same as the miniboson stars obtained in the system of the gravitational field and a massive complex scalar field. On the other hand, in the case of small breaking scale, $\eta/M_\mathrm{P} \ll 1$, the solutions are classified into three types: miniboson stars, matter-interacting NTS stars, and gravitating NTS stars. For the first type, gravity and a scalar field contribute the solutions in the same way as the large breaking-scale case. In the second type, interactions between matter fields are important as in the case of nontopological solitons discussed in Refs. [18–20]. In the last one, the both matter interaction and self-gravity are important, and NTS star solutions of this type can have much larger mass than other types. In the cases of miniboson stars and matter-interacting NTS stars, the gravity is weak because the lapse function is almost constant everywhere, while in the case of gravitating NTS stars, gravity requires a relativistic description where the lapse varies significantly.

We found that the maximum mass, which depend on the breaking scale, obeys a double power law: $M_* \propto \eta^{-1}$ for $\eta \gtrsim \eta_\mathrm{cr}$ and $M_* \sim \eta^{-2}$ for $\eta \lesssim \eta_\mathrm{cr}$, where $\eta_\mathrm{cr} \sim M_\mathrm{P}/3$. If we can extrapolate this for much lower breaking scale, the maximum mass of the NTS star can be astrophysical scale, the solar mass for $\eta \sim 1$ GeV and the cluster of galaxies scale for $\eta \sim 1$ eV.

We studied the compactness, the gravitational radius over the radius of the NTS stars. The compactness of NTS stars with maximum mass, C_*, takes the value $C_* \sim 0.167$ for $\eta \gg M_\mathrm{P}$ and $C_* \sim 0.553$ for $\eta \ll M_\mathrm{P}$, and C_* change in its value quickly around $\eta \sim 0.1 M_\mathrm{P}$. It means the NTS stars with maximum mass in the lower breaking scale are relativistically compact object that have the innermost stable circular orbits. Therefore, the NTS stars in the case $\eta \ll M_\mathrm{P}$ can be seeds of supermassive black holes.

It is an important to clarify the issue of the stability of the NTS stars. We would expect that the NTS stars with maximum mass evolve to black holes if they become unstable. Linear perturbation of the NTS stars would be our next work.

In this paper, we construct NTS star solutions whose internals are filled by kinetic energy of the scalar fields. These are self-gravitating solutions of dust balls [20]. There are other types of NTSs; potential balls and shell balls, in the model without gravity [20]. If we take gravity into account, a self-gravitating potential ball would be a 'gravastar' [37,38] that join de Sitter and Scwarzshild spacetimes by a spherical shell, and a self-gravitating shell ball would join Minkowski and Scwarzshild spacetimes [39]. It is also interesting to construct these solutions.

ACKNOWLEDGMENTS

We would like to thank K. -i. Nakao, H. Yoshino, and M. Minamitsuji for valuable discussions. This work was partly supported by Osaka Central Advanced Mathematical Institute: MEXT Joint Usage/Research Center on Mathematics and Theoretical Physics Grant No. JPMXP0619217849.

APPENDIX: ENERGY-MOMENTUM TENSOR AND CHARGE DENSITIES

Given the assumptions of the scalar and the gauge field forms, we can reduce the energy-momentum tensor (12) as

$$\begin{aligned} T^t_t/\eta^4 &= -\epsilon \\ &= -\frac{(e^2 f^2\alpha^2 + (e\alpha - \Omega)^2 u^2)}{\sigma^2(1-2m/r)} \\ &\quad - \left(1-\frac{2m}{r}\right)\left(\left(\frac{df}{dr}\right)^2 + \left(\frac{du}{dr}\right)^2\right) \\ &\quad - \frac{\lambda}{4}(f^2-1)^2 - \mu f^2 u^2 - \frac{1}{2\sigma^2}\left(\frac{d\alpha}{dr}\right)^2, \end{aligned} \tag{A1}$$

$$\begin{aligned} T^r_r/\eta^4 &= p_r \\ &= \frac{(e^2 f^2\alpha^2 + (e\alpha - \Omega)^2 u^2)}{\sigma^2(1-2m/r)} \\ &\quad + \left(1-\frac{2m}{r}\right)\left(\left(\frac{df}{dr}\right)^2 + \left(\frac{du}{dr}\right)^2\right) \\ &\quad - \frac{\lambda}{4}(f^2-1)^2 - \mu f^2 u^2 - \frac{1}{2\sigma^2}\left(\frac{d\alpha}{dr}\right)^2, \end{aligned} \tag{A2}$$

$$\begin{aligned} T^\theta_\theta/\eta^4 &= p_\theta = T^\varphi_\varphi/\eta^4 = p_\varphi \\ &= \frac{(e^2 f^2\alpha^2 + (e\alpha - \Omega)^2 u^2)}{\sigma^2(1-2m/r)} \\ &\quad - \left(1-\frac{2m}{r}\right)\left(\left(\frac{df}{dr}\right)^2 + \left(\frac{du}{dr}\right)^2\right) \\ &\quad - \frac{\lambda}{4}(f^2-1)^2 - \mu f^2 u^2 + \frac{1}{2\sigma^2}\left(\frac{d\alpha}{dr}\right)^2, \end{aligned} \tag{A3}$$

where ϵ represents an energy density of the fields, p_r and p_θ denote pressure in the direction of r and θ. We have the charge densities as

$$\rho_\psi = -2\sigma^{-2}\left(1-\frac{2m}{r}\right)^{-1} 2e(e\alpha-\Omega)u^2, \tag{A4}$$

$$\rho_\phi = -2\sigma^{-2}\left(1-\frac{2m}{r}\right)^{-1} e^2 f^2 \alpha. \tag{A5}$$

[1] G. Rosen, J. Math. Phys. (N.Y.) **9**, 996 (1968).
[2] S. R. Coleman, Nucl. Phys. **B262**, 263 (1985); Nucl. Phys. **B269**, 744(E) (1986).
[3] R. Friedberg, T. D. Lee, and A. Sirlin, Phys. Rev. D **13**, 2739 (1976).
[4] T. D. Lee and Y. Pang, Phys. Rep. **221**, 251 (1992).
[5] E. Y. Nugaev and A. V. Shkerin, J. Exp. Theor. Phys. **130**, 301 (2020).
[6] Y. M. Shnir, *Topological and Non-Topological Solitons in Scalar Field Theories* (Cambridge University Press, Cambridge, England, 2018).
[7] K. M. Lee, J. A. Stein-Schabes, R. Watkins, and L. M. Widrow, Phys. Rev. D **39**, 1665 (1989).
[8] X. Shi and X. Z. Li, J. Phys. A **24**, 4075 (1991).
[9] I. E. Gulamov, E. Y. Nugaev, A. G. Panin, and M. N. Smolyakov, Phys. Rev. D **92**, 045011 (2015).
[10] A. Kusenko and M. E. Shaposhnikov, Phys. Lett. B **418**, 46 (1998).
[11] A. Kusenko and P. J. Steinhardt, Phys. Rev. Lett. **87**, 141301 (2001).
[12] M. Fujii and K. Hamaguchi, Phys. Lett. B **525**, 143 (2002).

[13] K. Enqvist, A. Jokinen, T. Multamaki, and I. Vilja, Phys. Lett. B **526**, 9 (2002).

[14] A. Kusenko, L. Loveridge, and M. Shaposhnikov, Phys. Rev. D **72**, 025015 (2005).

[15] K. Enqvist and J. McDonald, Phys. Lett. B **425**, 309 (1998).

[16] S. Kasuya and M. Kawasaki, Phys. Rev. D **61**, 041301 (2000).

[17] M. Kawasaki, F. Takahashi, and M. Yamaguchi, Phys. Rev. D **66**, 043516 (2002).

[18] H. Ishihara and T. Ogawa, Prog. Theor. Exp. Phys. **2019**, 021B01 (2019).

[19] H. Ishihara and T. Ogawa, Phys. Rev. D **99**, 056019 (2019).

[20] H. Ishihara and T. Ogawa, Phys. Rev. D **103**, 123029 (2021).

[21] P. Forgács and Á. Lukács, Phys. Rev. D **102**, 076017 (2020).

[22] P. Forgács and Á. Lukács, Eur. Phys. J. C **81**, 243 (2021).

[23] D. J. Kaup, Phys. Rev. **172**, 1331 (1968).

[24] R. Ruffini and S. Bonazzola, Phys. Rev. **187**, 1767 (1969).

[25] M. Colpi, S. L. Shapiro, and I. Wasserman, Phys. Rev. Lett. **57**, 2485 (1986).

[26] P. Jetzer and J. J. van der Bij, Phys. Lett. B **227**, 341 (1989).

[27] A. B. Henriques, A. R. Liddle, and R. G. Moorhouse, Phys. Lett. B **233**, 99 (1989).

[28] A. B. Henriques, A. R. Liddle, and R. G. Moorhouse, Nucl. Phys. **B337**, 737 (1990).

[29] P. Jetzer, Phys. Rep. **220**, 163 (1992).

[30] F. E. Schunck and E. W. Mielke, Classical Quantum Gravity **20**, R301 (2003).

[31] S. L. Liebling and C. Palenzuela, Living Rev. Relativity **15**, 6 (2012).

[32] B. W. Lynn, Nucl. Phys. **B321**, 465 (1989).

[33] T. D. Lee, Phys. Rev. D **35**, 3637 (1987).

[34] R. Friedberg, T. D. Lee, and Y. Pang, Phys. Rev. D **35**, 3658 (1987).

[35] T. D. Lee and Y. Pang, Phys. Rev. D **35**, 3678 (1987).

[36] J. Kunz, V. Loiko, and Y. Shnir, Phys. Rev. D **105**, 085013 (2022).

[37] P. O. Mazur and E. Mottola, arXiv:gr-qc/0109035.

[38] P. O. Mazur and E. Mottola, Proc. Natl. Acad. Sci. U.S.A. **101**, 9545 (2004).

[39] B. Kleihaus, J. Kunz, C. Lammerzahl, and M. List, Phys. Lett. B **675**, 102 (2009).